



Published in final edited form as:

Funct Imaging Model Heart. 2023 June ; 13958: 74–83. doi:10.1007/978-3-031-35302-4_8.

On the possibility of estimating myocardial fiber architecture from cardiac strains

Muhammad Usman¹, Emilio A. Mendiola¹, Tanmay Mukherjee¹, Rana Raza Mehdi¹, Jacques Ohayon^{2,3}, Prasanna G. Alluri⁴, Sakthivel Sadayappan⁵, Gaurav Choudhary⁶, Reza Avazmohammadi^{1,3,7}

¹Department of Biomedical Engineering, Texas A&M University, College Station, TX 77843, USA

²Savoie Mont-Blanc University, Polytech Annecy-Chambéry, Le Bourget du Lac, France

³Department of Cardiovascular Sciences, Houston Methodist Academic Institute, Houston, TX 77030, USA

⁴Department of Radiation Oncology, UT Southwestern Medical Center, Dallas, TX 75390, USA

⁵Department of Internal Medicine, Division of Cardiovascular Health and Disease, University of Cincinnati College of Medicine, Cincinnati, OH 45267, USA

⁶Department of Medicine, Alpert Medical School of Brown University, Providence, RI 02903, USA

⁷J. Mike Walker '66 Department of Mechanical Engineering, Texas A&M University, College Station, TX, USA.

Abstract

The myocardium is composed of a complex network of contractile myofibers that are organized in such a way as to produce efficient contraction and relaxation of the heart. The myofiber architecture in the myocardium is a key determinant of cardiac motion and the global or organ-level function of the heart. Reports of architectural remodeling in cardiac diseases, such as pulmonary hypertension and myocardial infarction, potentially contributing to cardiac dysfunction call for the inclusion of an architectural marker for an improved assessment of cardiac function. However, the in-vivo quantification of three-dimensional myo-architecture has proven challenging. In this work, we examine the sensitivity of cardiac strains to varying myofiber orientation using a multiscale finite-element model of the LV. Additionally, we present an inverse modeling approach to predict the myocardium fiber structure from cardiac strains. Our results indicate a strong correlation between fiber orientation and LV kinematics, corroborating that the fiber structure is a principal determinant of LV contractile behavior. Our inverse model was capable of accurately predicting the myocardial fiber range and regional fiber angles from strain measures. A concrete understanding of the link between LV myofiber structure and motion, and the development of non-invasive and feasible means of characterizing the myocardium architecture is expected to lead to advanced LV functional metrics and improved prognostic assessment of structural heart disease.

Keywords

Myocardium architecture; left ventricle; cardiac strains; magnetic resonance imaging

1 Introduction

The intricate architecture of the underlying muscle fibers of the myocardium, often characterized by the three-dimensional orientation of the myofibers, plays a crucial role in the fundamental cardiac motion, regional stress and strain development (7; 11), and the pumping function of the left ventricle (LV) (16). Although the myocardium is designed to provide optimal contractile behavior in a healthy state, the fiber architecture may undergo remodeling events in the diseased heart (5). Myocardial architectural remodeling has been observed ex-vivo in a variety of structural heart diseases, including pulmonary hypertension (2; 10), cardiomyopathy (6), and myocardial infarction (14; 9). Therefore, it is necessary to develop an understanding of the relationship between cardiac structure and function and, ultimately, include the characterization of tissue architecture in the noninvasive assessment of cardiac diseases that involve biomechanical impairment of the myocardium. Moreover, in-vivo quantification of myo-architecture enables the calculation of cardiac fiber strain in lieu of “anatomical” strains, which holds the promise of improving early diagnosis of several cardiac diseases, including cancer treatment-related cardiotoxicity by early identification of motion impairments at the myofiber level.

Recent advances in cardiac imaging modalities have allowed for the characterization of the myocardial fiber structure from whole tissues, without the need for sectioning and histology. The study of the cardiac structure using diffusion-tensor magnetic resonance imaging (DT-MRI) has accelerated the relationship between cardiac architecture and function in health and disease. However, despite recent advances in in-vivo cardiac DT-MRI(13; 12), the need for additional sequencing and complex motion compensation processing to eliminate artifacts (15), a low spatial resolution, and poor accessibility have severely limited the application of cardiac DT-MRI in the clinical setting. These limitations are even more severe for small animal studies due to exasperated size, heart rate, and breath-control limits. As such, there is a need to develop methods to characterize the cardiac fiber structure from data that is easily quantified from traditional in vivo imaging techniques.

In this study, we hypothesize that regional motion anisotropy can be used to estimate fiber orientation in each region of the tissue wall and propose to estimate myofiber orientation from cardiac strains for which cine sequences have been already established and standardized in both humans and small animals (8). We used a finite-element (FE) model of the LV, reconstructed from MRI scans of a murine heart, to investigate the relationship between myocardium structural characteristics and cardiac strain as a forward problem. Next, we present an inverse modeling approach to estimate the transmural myofiber helicity and regional fiber angle using systolic strains as inputs. As an important feature of our model, we use regional and average anatomical stains on short-axis slices from MRI rendering our mode compatible with MRI-based strain quantification. Recent studies have shown a strong correlation between strain and fiber architecture in both forward and inverse problem manners (3; 4). In the present work, we focus on developing a subject-specific structure-strain pipeline that is compatible with standard cardiac MRI acquisitions where strains can be readily calculated from short-axis MRI scans. The results from this investigation will extend the present knowledge of the influence of myocardial structure on LV contractile behavior and indicate the possibility of developing methods to accurately

predict myofiber orientation measures from commonly available cardiac strain calculation modalities.

2 Materials and Methods

2.1 Left ventricle finite element model

The LV geometry used in this study was obtained from MRI scans of a healthy C57Bl/6 male mouse ($n=1$). An MRI scan was acquired using a 7T Biospec system (Bruker, Billerica, MA). The imaging protocol was approved by the University of Cincinnati's Animal Care and Use Committee. A FE model of the LV was used in this study to perform forward- and inverse-model investigations of the relationship between ventricular strain and myocardial fiber architecture. Briefly, the construction of the model consisted of three main steps: (i) reconstruction (using end-diastole time point) and meshing of the 3-D ventricular geometry (using linear tetrahedral elements), (ii) assigning myofiber architecture to the FE mesh, and (iii) incorporating the passive and active constitutive laws. Detailed methods regarding model development were described previously (1). Our development approach resulted in an animal-specific multiscale model of the LV capable of reproducing expected kinematic behavior during diastole and systole. Several *in-silico* experiments were conducted with the completed LV model to investigate the sensitivity of cardiac strains to myofiber architecture, followed by an inverse modeling study to predict the fiber architecture from myocardial strains.

To investigate the myocardium fiber architecture effect on cardiac strains, synthetic fiber structures were developed for the LV model and used in forward simulations of the cardiac cycle. The resulting predicted strain data was then plotted against metrics describing the myofiber structure to determine the relationship between strain and fiber architecture. Next, an inverse model was developed to attempt to predict the myofiber architecture from cardiac strains. Finally, the effect of various fiber structures on ventricular torsion, a promising metric of LV function, was performed.

2.2 Development of synthetic fiber architectures

A set of synthetic fiber architectures was created for the LV model. As part of the model development, a simple Laplace-Dirichlet boundary-value problem, using fixed values at the endo- and epicardial surfaces, was used to determine three layers spanning the transmural direction of the LV wall were determined: endocardium, midwall, and epicardium. An artificial architecture was constructed by defining a linear transmural transition between the chosen fiber angles in the epicardial (θ_{epi}) and endocardial (θ_{endo}) layers (Fig. 1a). The synthetic architectures were developed, ensuring the endocardium fiber angle was between 0° and 82° , and the epicardium fiber angle was between 0° and -62° . Fiber range was used in this work as a metric of LV fiber helicity and defined as $(\theta_{endo} - \theta_{epi})$.

2.3 Relationship between fiber-orientation and strains: Forward problem

To determine the relationship between cardiac strains and fiber orientation, *in-silico* experiments were conducted in which a synthetic fiber structure was mapped to the LV model, and a forward simulation of the cardiac cycle was completed. Average strains at the

end-systolic (ES) point in the simulated cardiac cycle were calculated on four short-axis slices of the ventricle acquired in the MRI scan (Fig 1b). The slices were labeled as base, mid, apical, and apex. The Green-Lagrange strain at ES was calculated as:

$$\mathbf{E} = \frac{1}{2}(\mathbf{F}^T \mathbf{F} - \mathbf{I}), \quad (1)$$

where \mathbf{I} is the identity matrix, and \mathbf{F} is the deformation gradient. The strains were transformed from a global coordinate system to the common {circumferential, radial, longitudinal} coordinates using:

$$\mathbf{E}_{C,R,L} = \mathbf{Q}\mathbf{E}\mathbf{Q}^T, \quad (2)$$

where C, R, L subscripts refer to circumferential, radial, and longitudinal axes, respectively, and \mathbf{Q} is a transformation matrix to transform the strains from global coordinates to anatomical coordinates. We first studied the correlation between full-thickness averages of $\mathbf{E}_{C,R,L}$ across the base, mid, and apical short-axis slices (Fig. 1b) and the fiber range. Next, slices were divided into three transmural layers, namely, epicardial, mid, and endocardial layers, to study the correlation between regional strains and fiber angle at respective layers.

2.4 Relationship between fiber-orientation and strains: Inverse problem

An inverse modeling approach was used to estimate the fiber range from simulated cardiac strains. An initial forward simulation with a synthetic fiber structure was conducted. Strains calculated on the top three short-axis slices were then used as target “ground-truth” for the inverse problem. A nonlinear least-squares regression, using Trust Region Reflective algorithm, was used to estimate the fiber orientations in terms of the helical angles θ_{epi} and θ_{endo} assuming a linear transition from θ_{endo} to θ_{epi} . The inverse problem iteratively ran forward simulations to minimize the collective errors between the “ground-truth” strains and predicted strains. The residual error between ground-truth and predicted strains at each iteration was defined by:

$$r_i = E_i^{true} - E_i^{pred}, \quad i = C, R, L, \quad (3)$$

where E^{true} and E^{pred} are ground-truth and predicted strains, respectively. The objective function set to be minimized was defined as the sum of all residual errors:

$$\phi = \sum_{j=1}^{N_S} r_C^2 + \sum_{j=1}^{N_S} r_R^2 + \sum_{j=1}^{N_S} r_L^2, \quad (4)$$

where j represents the number of the slices (N_S), including the base, mid, apical, and apex. Following the correlation results from our forward problem (described in 3.1 and 3.2), whole or certain terms of the objective function providing minimal errors were used in the inverse problem.

3 Results

3.1 Strains were correlated with fiber orientation

In this study, the results are presented for the fiber range spanning from 106 to 146 degrees. This fiber range was created with the endocardial fiber angle being fixed at 84 degrees and the epicardial fiber angle changing from -22 and -62 degrees. Strains were calculated and averaged within the top three short-axis slices (base, mid, and apical). The correlation between the average strain and fiber range for three of the slices is presented in Fig. 2. The results indicate that circumferential and longitudinal strains are highly negatively correlated with fiber range. Radial strains exhibited a strong positive correlation with the fiber range. Interestingly, the strain ranges tended to decrease moving from the base to the apex. The radial strains showed the best correlation between fiber range and strain at all three slices (Fig. 2).

3.2 Fiber architecture influences regional strain

A strong correlation was observed between fiber angle and regional strain at all three slices. A representative example of the correlations is displayed for the mid slice (Fig. 3). Correlation trends similar to those in Fig. 2 were observed between regional fiber angle and strains in the endo- and epicardium layers: absolute circumferential and longitudinal strains in each layer tended to increase as the fiber angle moves away from the circumferential direction (Fig. 3). Similar correlation results were also noted in the other short-axis slices. We note that our small strain magnitudes (compared to commonly reported ranges of myocardial strains) are due to a lower systolic pressure used in the LV to facilitate forward and inverse model simulations.

3.3 Prediction of myofiber angle from cardiac strains

The results of the forward problem in Figs. 2 and 3 confirmed a very strong relationship between cardiac strains and the myocardial fiber structure. Two separate inverse problems were conducted: (i) the estimation of fiber range from average fiber strain on each short-axis slice, and (ii) the estimation of regional fiber angle from respective regional strains. Our inverse modeling approach exhibited a strong predictive correlation between the ground-truth and estimated fiber range values (Fig. 4) corroborating the capability of the model to accurately predict fiber range from average strains. Also, the inverse model made an accurate estimation of the endo- and epicardium regional fiber angle (Fig. 5), with no significant difference between the mean ground truth and predicted fiber angles.

4 Discussion and Conclusions

Myocardial fiber architecture is known to have a principal influence on LV kinematics and, thus, organ-level cardiac function. The myocardium structure is intricately designed to produce efficient contractile behavior; however, the fiber architecture often undergoes remodeling events as a result of cardiac disease. Metrics currently used in the prognosis and treatment of structural heart diseases (such as ejection fraction and relaxation time) offer global information on the state of LV function but may fail to promptly risk-stratify heart disease patients due to their limited sensitivity to tissue-level adaptations. As architectural

remodeling may offer indications of the trajectory of the disease, they offer significant added value to traditional metrics such as LV ejection fraction. However, the in-vivo and high-fidelity quantification of myofiber architecture has proven challenging, prompting alternative approaches to quantify myofiber architecture.

In the present study, we investigated the relationship between cardiac strains and myofiber structure and showed architectural metrics can be accurately predicted from kinematic data using FE modeling of a murine heart. Correlation analysis between fiber orientation and cardiac strains indicated a strong association at various short-axis slices of the ventricle. Similarly, regional strains and fiber angles in distinct transmural regions of the LV were found to be highly correlated. Both these results indicate the myofiber architecture of the ventricle exerts a heavy influence on the contractile pattern of the healthy LV. Thus, it is important to develop methods to characterize the myofiber architecture of the LV non-invasively. The inverse problem approach we used to estimate architectural metrics were able to accurately predict both fiber range and regional fiber angles from cardiac strains. This promising result suggests such a method could be developed to make use of strains measured on short-axis slices of the LV in commonly used in-vivo imaging techniques, such as cardiac MRI and echocardiography.

While this study presents a promising approach to predict myocardial fiber orientation from cardiac strains, further developments are needed for translating this approach for pre-clinical and clinical applications. Here, synthetic data was used to generate the fiber orientation. While this allowed us to feasibly investigate the correlation between fiber orientation and cardiac strains in a forward problem manner, the ground truth was chosen from prescribed orientations to validate the model in an inverse problem setting. In future studies, the cardiac strains will be taken from in-vivo imaging, and predicted fiber angles will be compared against ground-truth fiber orientation measured in-vivo or ex-vivo. Moreover, our study was restricted to one healthy LV model that could be extended both in terms of sample size and the structural heart diseases known to induce architectural remodeling. Furthermore, the performance of (R, C, L) strains compared to shear strains with respect to predicting fiber orientation remains to be investigated.

Overall, we have shown here that the structure of the myocardium is a principal determinant of LV contractile motion, and a rigorous inverse model can be established between the structure and motion. We presented a version of such an inverse model that is compatible with common anatomical strain calculations from standard cine cardiac MRI acquisitions. Further investigation of this approach may result in the establishment of a feasible technique to noninvasively estimate myofiber orientation and helicity using routinely available cardiac imaging in both small animals and humans. Ultimately, such structurally-informed functional metrics could provide detailed supplemental information to the traditional gross metrics of LV function and improve prognostic and therapeutic assessments. Finally, as LV torsion has recently been introduced as a promising kinematic metric of LV functional capacity, we suggest that further studies include the association between fiber architecture and torsion. Ventricular torsion, also readily quantified from standard imaging studies, may provide another avenue to link the myocardium structure with LV kinematics.

Acknowledgements

This research was supported by the NIH Grant No. R00HL138288 to R.A..

References

- [1]. Avazmohammadi R, Mendiola EA, Soares JS, Li DS, Chen Z, Merchant S, Hsu EW, Vanderslice P, Dixon R, Sacks M: A Computational Cardiac Model for the Adaptation to Pulmonary Arterial Hypertension in the Rat. *Annals of Biomedical Engineering* 47(1), 138–153 (09 2019). 10.1007/s10439-018-02130-y [PubMed: 30264263]
- [2]. Avazmohammadi R, Hill M, Simon M, Sacks M: Transmural remodeling of right ventricular myocardium in response to pulmonary arterial hypertension. *APL bioengineering* 1(1), 016105 (2017) [PubMed: 30417163]
- [3]. Barbarotta L, Bovendeerd PH: A computational approach on sensitivity of left ventricular wall strains to fiber orientation. In: *Functional Imaging and Modeling of the Heart: 11th International Conference, FIMH 2021, Stanford, CA, USA, June 21–25, 2021, Proceedings*. pp. 296–304. Springer (2021)
- [4]. Barbarotta L, Bovendeerd PH: Parameter estimation in a rule-based fiber orientation model from end systolic strains using the reduced order unscented kalman filter. In: *Functional Imaging and Modeling of the Heart: 11th International Conference, FIMH 2021, Stanford, CA, USA, June 21–25, 2021, Proceedings*. pp. 340–350. Springer (2021)
- [5]. Buckberg G, Hoffman JI, Mahajan A, Saleh S, Coghlan C: Cardiac mechanics revisited: the relationship of cardiac architecture to ventricular function. *Circulation* 118(24), 2571–2587 (2008) [PubMed: 19064692]
- [6]. Ferreira PF, Kilner PJ, McGill LA, Nielles-Vallespin S, Scott AD, Ho SY, McCarthy KP, Haba MM, Ismail TF, Gatehouse PD, et al. : In vivo cardiovascular magnetic resonance diffusion tensor imaging shows evidence of abnormal myocardial laminar orientations and mobility in hypertrophic cardiomyopathy. *Journal of Cardiovascular Magnetic Resonance* 16(1), 1–16 (2014) [PubMed: 24387349]
- [7]. Geerts L, Kerckhoffs R, Bovendeerd P, Arts T: Towards patient specific models of cardiac mechanics: a sensitivity study. In: *International Workshop on Functional Imaging and Modeling of the Heart*. pp. 81–90. Springer (2003)
- [8]. Keshavarzian M, Fugate E, Chavan S, Chu V, Arif M, Lindquist D, Sadayappan S, Avazmohammadi R: An image registration framework to estimate 3d myocardial strains from cine cardiac mri in mice. In: *Functional Imaging and Modeling of the Heart: 11th International Conference, FIMH 2021, Stanford, CA, USA, June 21–25, 2021, Proceedings*. pp. 273–284. Springer (2021)
- [9]. Mendiola E, Neelakantan S, Xiang Q, Merchant S, Li K, Hsu E, Dixon R, Vanderslice P, Avazmohammadi R: Contractile adaptation of the left ventricle post-myocardial infarction: Predictions by rodent-specific computational modeling. *Ann Biomed Eng* 16(2), 721–729 (2022)
- [10]. Mendiola EA, da Silva Gonçalves Bos D, Leichter DM, Vang A, Zhang P, Leary OP, Gilbert RJ, Avazmohammadi R, Choudhary G.v: Right ventricular architectural remodeling and functional adaptation in pulmonary hypertension. *Circulation: Heart Failure* 16(2), e009768 (2023) [PubMed: 36748476]
- [11]. Pluijmert M, Delhaas T, de la Parra AF, Kroon W, Prinzen FW, Bovendeerd PH: Determinants of biventricular cardiac function: a mathematical model study on geometry and myofiber orientation. *Biomechanics and modeling in mechanobiology* 16(2), 721–729 (2017) [PubMed: 27581324]
- [12]. Scott AD, Nielles-Vallespin S, Ferreira PF, Khaliq Z, Gatehouse PD, Kilner P, Pennell DJ, Firmin DN: An in-vivo comparison of stimulated-echo and motion compensated spin-echo sequences for 3 t diffusion tensor cardiovascular magnetic resonance at multiple cardiac phases. *Journal of Cardiovascular Magnetic Resonance* 20(1), 1–15 (2018) [PubMed: 29298692]
- [13]. Stoeck CT, Von Deuster C, Genet M, Atkinson D, Kozerke S: Second-order motion-compensated spin echo diffusion tensor imaging of the human heart. *Magnetic resonance in medicine* 75(4), 1669–1676 (2016) [PubMed: 26033456]

- [14]. Walker JC, Guccione JM, Jiang Y, Zhang P, Wallace AW, Hsu EW, Ratcliffe MB: Helical myofiber orientation after myocardial infarction and left ventricular surgical restoration in sheep. *The Journal of thoracic and cardiovascular surgery* 129(2), 382–390 (2005) [PubMed: 15678050]
- [15]. Welsh CL, DiBella EV, Hsu EW: Higher-order motion-compensation for in vivo cardiac diffusion tensor imaging in rats. *IEEE transactions on medical imaging* 34(9), 1843–1853 (2015) [PubMed: 25775486]
- [16]. Zhang X, Haynes P, Campbell KS, Wenk JF: Numerical evaluation of myofiber orientation and transmural contractile strength on left ventricular function. *Journal of biomechanical engineering* 137(4), 044502 (2015) [PubMed: 25367232]

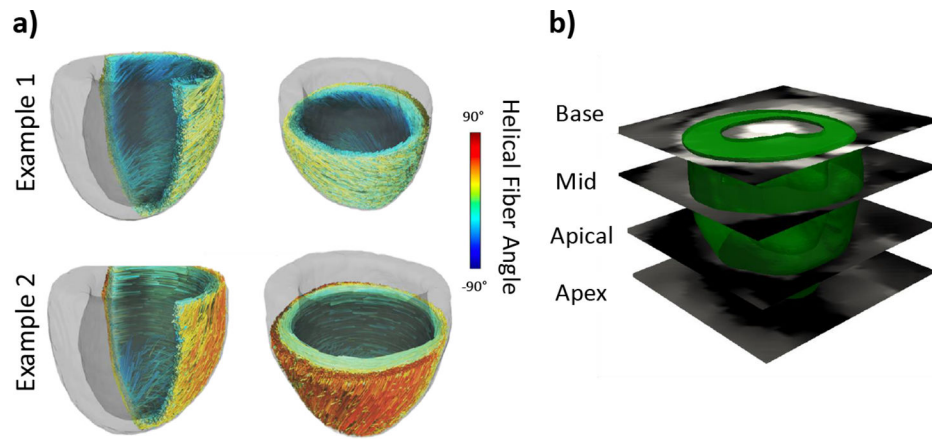


Fig. 1:

- (a) Examples of synthetic fiber structures with helical fiber angle ranging from -90° to 90° .
(b) Short-axis slices on which strains were calculated.

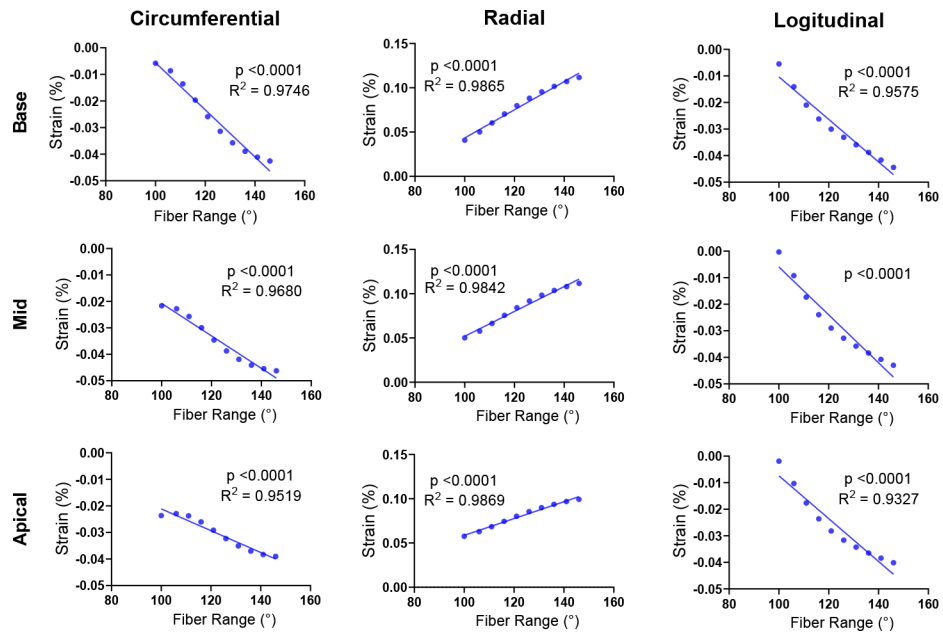


Fig. 2: Correlation analysis between full-thickness average cardiac strains and the transmural fiber range at the base, mid, and apical slices.

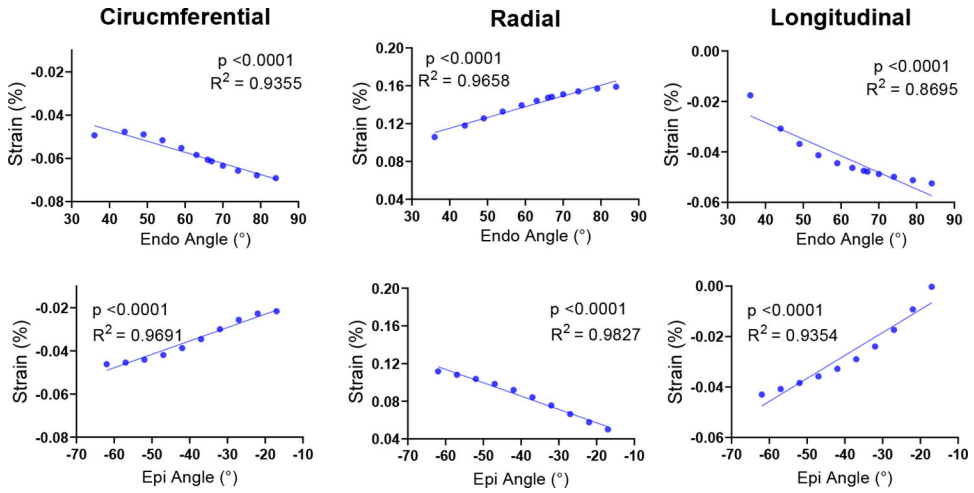


Fig. 3: Correlation analysis between the regional strains and the local fiber angle in the respective transmural layer. This analysis was performed with strains calculated at the epicardial and endocardial layers of the Mid short-axis slice.

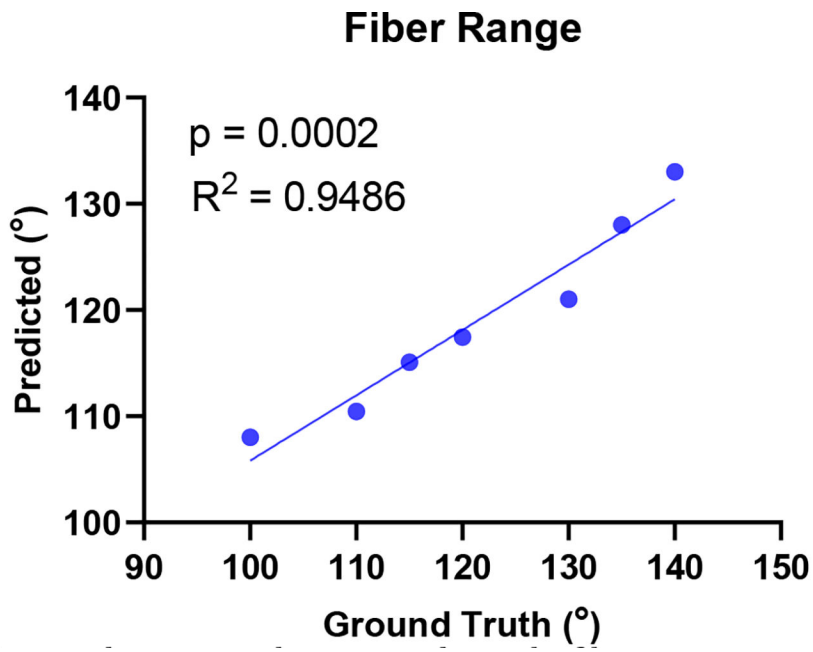


Fig. 4: Correlation between the ground-truth fiber range and the fiber range predicted by inverse modeling.

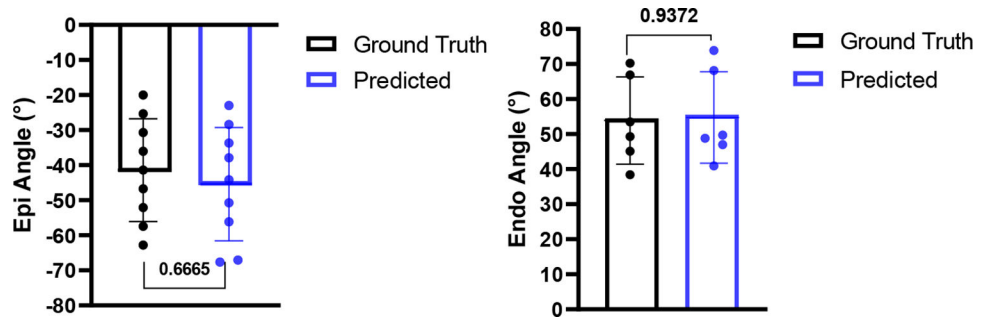


Fig. 5:
Inverse modeling resulted in an accurate prediction of endocardium and epicardium fiber angle from cardiac strains.

Author Manuscript

Author Manuscript

Author Manuscript

Author Manuscript